SURE 静岡大学学術リポジトリ
Shizuoka University REpository

Isolation and structure determination of new siderophore albachelin from Amycolatopsis alba

メタデータ	言語: eng 出版者: 公開日: 2016-12-26 キーワード (Ja): キーワード (En): 作成者: Kodani, Shinya, Komaki, Hisayuki, Suzuki, Masahiro, Hemmi, Hikaru, Ohnishi-Kameyama, Mayumi メールアドレス: 所属:
URL	http://hdl.handle.net/10297/9931

Biometals, full paper

Title: Isolation and structure determination of new siderophore albachelin from *Amycolatopsis alba*

Authors: Shinya Kodani[*,1], Hisayuki Komaki[2], Masahiro Suzuki[1], Hikaru Hemmi[3], Mayumi Ohnishi-Kameyama[3]

Affiliations and addresses:

[1]Graduate School of Agriculture, Shizuoka University, Shizuoka University, 836 Ohya, Suruga-ku, Shizuoka 422-8529, Japan

[2]Biological Resource Center, National Institute of Technology and Evaluation (NBRC), 2-5-8 Kazusakamatari, Kisarazu, Chiba 292–0818, Japan

[3]National Food Research Institute, National Agriculture and Food Research Organization (NARO), 2–1-12 Kannondai, Tsukuba, Ibaraki 305-8642, Japan

***To whom correspondence should be addressed:** Shinya Kodani, Graduate School of Agriculture, Shizuoka University, 836 Ohya, Suruga-ku, Shizuoka 422-8529, Japan, Tel/Fax; +81(54)238-5008, E-mail; kodani.shinya@shizuoka.ac.jp

Abstract

A new siderophore named albachelin was isolated from iron deficient culture of *Amycolatopsis alba*. The planar structure of albachelin was elucidated by the combination of ESI-MS/MS experiment and NMR spectroscopic analyses of the gallium (III) complex. The structure of albachelin was determined to be a linear peptide consisting of 6 mole of amino acids including 3 mole of serine, one mol each of *N*-α-acethyl-*N*-δ-hydroxy-*N*-δ-formylornithine, *N*-α-methyl-*N*-δ-hydroxyornithine, and cyclic *N*-hydroxyornithine. The stereochemistries of amino acids constituting albachelin were analyzed by applying modified Marfey method to the hydrolysate of albachelin. Based on bioinformatics, we deduced and discussed the possible biosynthetic gene cluster involved in albachelin biosynthesis from the genome sequence of *A. alba*. By prediction of substrates for adenylation domains, a non-ribosomal peptide biosynthetase gene (AMYAL_RS0130210) was proposed to be the main biosynthetic gene for albachelin biosynthesis. The related genes including transporter for siderophore were found near the NRPS gene as a gene cluster.

Keywords: siderophore, *Amycolatopsis alba*, peptide, biosynthesis

Introduction

Recent genome sequencing of actinomycetes has now indicated that the genome of each strain contains multiple biosynthetic gene clusters which are predicted to encode the assembly-line biosynthesis of polyketides or nonribosomal peptides (Clardy 2006; Komaki et al. 2014; Komaki et al. 2012; Zerikly and Challis 2009). According to development of bioinformatics and accumulation of biosynthetic gene data, the structural prediction of natural products has been possible from biosynthetic genes predicted by the genome-mining (Bachmann and Ravel 2009; Rottig et al. 2011). However under normal culture conditions, many of these gene clusters are not expressed enough to produce the resulting compounds (Ochi and Hosaka 2013), and therefore it is claimed that genome resources of actinomycetes remain unexploited although secondary metabolite biosynthetic genes exist abundantly in their genomes and possess a wide diversity.

In iron deficient condition, some bacteria secrete siderophores which are defined as small molecular weight compounds with high-affinity of iron chelating (Ahmed and Holmstrom 2014). According to the biosynthetic system, siderophores have been classified into two groups including one NRPS (Non Ribosomal Peptide Synthesis) dependent (Crosa and Walsh 2002) such as ferrichrome (Mercier and Labbe 2010) and the other NRPS independent (Challis 2005) such as desferrioxamine (Barona-Gomez et al. 2004). The NRPS protein is mostly a large molecular multi-enzyme which functions as the assembly-line to produce the resulting peptide through a series of amino acid building modules lined up in parallel (Sieber and Marahiel 2005). Each module in NRPS causes successive elongation of the peptide by one amino acid with enzymatic function of condensation (C) domain. Each module normally contains a basic set of

59 three domains, an adenylation (A) domain for the recognition of specific amino acid substrate, a
60 peptidyl carrier protein (PCP) that binds the growing peptide chain and the incoming aminoacyl
61 unit, and a C domain to catalyze peptide bond formation between amino acids on neighboring
62 PCPs. Optional domains such as epimerization (E) and *N*-methylation (MT) domains sometimes
63 exist on the modules and modify amino acid to afford unnatural amino acid such as D-amino
64 acid and *N*-methyl amino acid. A thioesterase (TE) domain normally exists at the end of
65 assembly-line of NRPS to release full-length of the peptide.
66 The A domain of NRPS in siderophore biosynthesis has been indicated to have high specificity
67 to amino acid substrate (Challis et al. 2000). Therefore structural prediction of siderophores has
68 comparatively been accomplished rather than other classes of NRPS biosynthesized peptides. A
69 siderophore coelichelin was the first example of structure-predicated peptide (Challis and Ravel
70 2000), and the structure elucidation of coelichelin revealed an unique NRPS system in which one
71 module is reused and others are skipped (Lautru et al. 2005). Erythrochelin was also isolated and
72 structure-elucidated based on genome mining of *Saccharopolyspora erythraea* (Robbel et al.
73 2010), and the function of NRPS was determined by gene disruption (Lazos et al. 2010). A new
74 siderophore biosynthesized by NRPS was found and isolated from *Streptomyces peucetius* based
75 on genome mining (Park et al. 2013). Recently, we isolated and structure-elucidated siderophore
76 scabchelin from plant-pathogen *S. scabies*, and found the biosynthetic gene cluster in its genome
77 (Kodani et al. 2013a). An unusual mixed-ligand siderophore amychelin was isolated from
78 *Amycolatopsis* sp. AA4 and its biosynthetic gene cluster was determined by whole genome
79 sequencing (Seyedsayamdost et al. 2011). Above all, isolation and structural elucidation of new
80 siderophores from bacteria whose genome sequence was determined gave the new insights of
81 biosynthetic genes by applying bioinformatics. On the basis of these circumstances, we isolated

82 a new siderophore named albachelin from type strain of *Amycolatopsis alba*, and the structure
83 was determined by the interpretation of NMR and MS spectra. Using bioinformatics with the
84 whole genome data of *A. alba*, the possible biosynthetic genes were deduced and discussed.

85 **Results**

86 In the course of screening for siderphore production, we found that *Amycolatopsis alba* (type
87 strain, JCM 10030) produced a siderophore on iron-deficient culture condition. Following the
88 method in previous paper (Kodani et al. 2013b), cultivation of *A. alba* was performed using 2L
89 of iron deficient media. To avoid the contamination of ferric ion, flasks and funnels made of
90 polystyrene were used to culture and harvest. After cultivation for 7 days, the bacterial cells
91 were removed from the culture media by filtration. 1M $FeCl_3$ solution (1 mL) was added to the
92 spent culture media to generate the complex of siderophore with ferric ion. The culture media
93 was concentrated to the aqueous solution up to 50 mL by rotary evaporator. The concentrated
94 material was subjected to open column chromatography using hydrophobic resin CHP-20P with
95 elution of 10% MeOH, 60% MeOH, and MeOH. The 60% MeOH fraction was subjected to
96 HPLC purification to yield 8.2 mg of the ferri-albachelin (Fe-albachelin). The measurement of
97 ESI-TOF mass spectrum of ferri-albachelin gave an ion peak at *m/z* 789.3. Since the presence of
98 ferric ion is not compatible with the NMR spectroscopy analysis, the conversion of the ferric
99 siderophore into gallium ion complex via desferri-albachelin was performed following previous
100 report (Kodani et al. 2013a; Kodani et al. 2013b). As a result, desferri-albachlin (**1** in Fig. 1) and
101 gallium-complex of albachelin (Ga-albachelin) were obtained with the yield of 1.0 and 4.0 mg,
102 respectively. After HPLC purification, the presence of Ga-albachelin was determined by ESI-
103 TOF MS analysis, which gave ion peaks at *m/z* 802.6 and 804.6 with intensity ratio of 6:4, which
104 indicated gallium complex.

Desferri-albachlin (**1**) was isolated as a white powder after lyophilization, and the molecular formula of **1** was determined to be $C_{28}H_{49}N_9O_{14}$ by FT-ICR ESI-MS analysis (*m/z* calculated for $C_{28}H_{50}N_9O_{14}^+$: 736.3471 found: 736.3476 for $[M+H]^+$). The analyses of NMR spectra including ^1H, ^{13}C, DEPT-135, DQF-COSY, TOCSY, NOESY, HMBC, HSQC, and ^1H-^{15}N HSQC were performed on Ga-albachelin dissolved in 0.5 mL of DMSO-d_6. The ^1H NMR spectral data showed peptidic characteristic with peaks of several amide residues over 8-9 ppm and α-protons over 4-5 ppm. By the interpretation of DQF-COSY and TOCSY, proton spin system of each amino acid was constructed as shown by bold line in Fig. 2a. The assignments of C-H spin system were performed by the interpretation of HSQC data (Table 1), and revealed that albachelin consisted of 6 mole of amino acids including 3 mole of Ser and one mol each of N-α-acethyl-*N*-δ-hydroxy-*N*-δ-formylornithine (*N*-Ac hfOrn), *N*-α-methyl-*N*-δ-hydroxyornithine (*N*-Me hOrn), and cyclic *N*-hydroxyornithine (chOrn). The existence of an acetyl residue was confirmed by the HMBC correlation from methyl protons (1.83 ppm) to carbonyl carbon (169.1 ppm). The HMBC correlation from amide proton (7.62 ppm) to the same carbonyl carbon (169.1 ppm) indicated that acetyl residue attached to amide proton of *N*-Ac hfOrn1. The presence of formyl residue was indicated by HSQC correlation from singlet proton (7.99 ppm) to characteristic chemical shift value of 152.2 ppm. The formyl residue was indicated to be attached to δ position in *N*-Ac hfOrn, by the HMBC correlation from δ-protons (3.29 and 3.49 ppm) to carbonyl carbon (152.2 ppm). As shown in Fig. 2a by one end arrow, the HMBC correlations from α-proton or amide proton to carboxyl carbon were used to establish the connections between *N*-Ac hfOrn1/Ser2, Ser4/Ser5, and Ser5/chOrn6. As shown in Fig. 2a by double end arrow, the NOESY correlation between α-proton of Ser2 and δ-protons of *N*-Me hOrn3 indicated the connection between Ser2 and *N*-Me hOrn3. The NOESY correlation

between α-proton of *N*-Me hOrn3 and amide proton of Ser4 indicated the connection between *N*-Me hOrn3 and Ser4. The hydroxyl residues in *N*-Ac hfOrn1, N-Me hOrn3 and chOrn6 were not detected by ^{1}H NMR, however the result of ESI-MS/MS experiment supported the positions of hydroxyl residues indicated in Fig. 2b. In ESI-MS/MS analyses of albachelin, the *b*-series of product ions at *m/z* 606 ($[M+H-130]^{+}$), 519 ($[M+H-130-87]^{+}$), 432 ($[M+H-130-87-87]^{+}$), 288 ($[M+H-130-87-87-144]^{+}$), and 201($[M+H-130-87-87-144-87]^{+}$) were observed The observed neutral losses of 130, 87, 144 correspond to those expected for chOrn, serine, and *N*-Me hOrn, respectively, further corroborating the results of the NMR spectroscopic analyses. The *y*-series product ion peaks were observed at *m/z* 536, 449, 305, and 208, which also confirmed the sequence of the peptide as shown in Fig. 2b. Above all, the structure of albachelin was determined as **1** in Fig. 1.

To elucidate the absolute stereochemistries of amino acids, the hydrolysate of ferri-albachelin was derivatized with *N*α-(5-fluoro-2,4-dinitrophenyl)-L-leucinamide (L-FDLA), and the derivative was subjected to HPLC analysis to compare with the standard amino acid derivatives with L-FDLA or D-FDLA (Harada et al. 1996). To obtain Orn and *N*-Me Orn, hydrogen iodide (HI) was used for hydrolysis with reduction. Regarding HPLC analysis for streochemistries of Ser residues, 2 mole of L-Ser and 1 mol of D-Ser were detected. Although 2 mole of L-Ser and 1 mol of D-Ser were indicated to be contained in the molecule, the specific positions of L- and D-Ser in the molecule were not determined. As for Orn, 1 mol each of L- and D-Orn was detected, however the specific positions of L- and D-Orn in the molecule were also not determined. The remaining amino acid, *N*-Me Orn was determined to be L-form, since only L-*N*-Me Orn was detected by HPLC analysis.

Discussion

We searched the albachelin biosynthetic gene cluster in the complete genome sequence of *A. alba* type strain (DSM 44262) recently released in public (GenBank accession number ARAF00000000.1), and found an NRPS gene cluster shown in Fig. 3a and Table S1. Most of the proteins encoded in the cluster are homologous to those in gene clusters for erythrochelin, coelichelin and scabichelin, which are siderophores structurally related to albachelin (Table S1). The large NRPS protein (7406 amino acids, AMYAL_RS0130210) comprised 6 modules composed of 21 domains, each module containing a set of C, A, and PCP domains essential for NRPS modules (Fig. 3b). This suggested the NRPS product to be a hexapeptide. To predict amino-acid substrates recognized by A domains in the NRPS, we compared the substrate specificity-determining residues with those of NRPSs for coelichelin, erythrochelin and scabichelin synthesis. Consequently, A domain of module 1 was predicted to recognize hfOrn based on the similarities (Table 2). A domains of modules 2, 4 and 5, and those of modules 3 and 6 were indicated to recognize Ser and hOrn, respectively. As optional domains, module 3 contained an MT domain, suggesting that hOrn3 within the hexapeptide is *N*-methylated. In addition, modules 2 and 6 of the NRPS contained an E domain each, suggesting that absolute stereochemistry of the Ser2 and hOrn6 is D-form. These predicted amino-acid building blocks completely corresponded to those of albachelin. Upstream of the NRPS, two genes encoding lysine/ornithine *N*-monooxygenases and formyltransferase were present (AMYAL_RS0130205 and AMYAL_RS0130200), which are essential for biosynthesis of L-hOrn and L-hfOrn, respectively. Downstream of the NRPS, AMYAL_RS0130220 and AMYAL_RS0130225 to AMYAL_RS0130245 encoded MbtH-like protein and proteins for ferric-siderophore export/uptake, respectively (Table S1). These results strongly suggested this gene cluster to be responsible for albachelin synthesis.

Regarding biosynthesis of unusual amino acids including L-hOrn and L-hfOrn, a flavin-dependent monooxygenase encoded by AMYAL_RS0130205 initially catalyzes *N*5-hydroxylation of L-Orn (Fig. 3b). The L-hOrn molecules are not only directly recognized by A domains of modules 3 and 6 as the building blocks, but also undergoes *N*5-formylation catalyzed by the formyltransferase encoded by AMYAL_RS0130200 yielding L-hfOrn, as reported in the biosynthesis of coelichelin (Lautru et al. 2005) and scabichelin (Kodani et al. 2013a). Each amino-acid building block (L-hfOrn for module 1, L-hOrn for modules 3 and 6, Ser for modules 2, 4, 5) is converted to aminoacyl adenylate by each the A domain, and transferred on to the adjacent PCP domain within each module to form the corresponding aminoacyl thioesters. When L-hfOrn is loaded onto module 1, the C domain catalyzes acetylation yielding *N*-Ac hfOrn according to the mechanism reported in erythrochelin synthesis (Robbel et al. 2010). L-hOrn loaded onto module 3 undergoes *N*-metylation by the MT domain. The L-Ser residue of module 2 and L-hOrn residue of module 6 undergo α-carbon epimerization catalyzed by the E domain within each module, and then C domains of modules from 2 to 6 catalyze five successive *N*-acylation reactions to yield a L, D, L, L, L, D - hexapeptidyl thioester attached to the PCP domain of module 6. The stereochemistry of three Ser residues in albachelin was expected to be D-form at Ser2 and L-forms at Ser4 and Ser5, although specific positions of two L- and one D-Ser residues in albachelin were not determined in the present study. However we detected L-Ser and D-Ser from hydrolysate of albachelin at the ratio of 2:1 by modified Merfey method, which corresponds to the speculation. In the same way, we detected L-Orn and D-Orn at the ratio of 1:1, which also seems to be reasonable, considering that *N*-Ac Orn1 and chOrn6 should biosynthetically be L- and D-forms. The remaining amino acid, *N*-Me Orn3 was determined to be L-form, which also agrees with the speculation. Interestingly, the NRPS of albachelin lacks

C-terminal TE domain as same as that of scabchelin (Kodani et al. 2013a). In the case of biosynthesis of structurally related siderophore amychelin which has chOrn residue at C-terminal, a putative standalone α,β-hydrolase (AmcB) was proposed to get involved in final release of peptide. (Seyedsayamdost et al. 2011) In *A. alba* genome, AMYAL_RS0125485 (WP_020634094) near the albachelin biosynthetic gene cluster encode a protein with 48% sequence identity (61% sequence similarity) to AmcB, suggesting likely to be an α,β-hydrolase. Hence, the putative α,β-hydrolase may catalyze final peptide chain release. Above all, we concluded that the NRPS gene cluster (Figure 3a) including main biosynthetic NRPS gene (AMYAL_RS0130210) was reasonably be the gene cluster of albachelin biosynthesis.

Materials and Methods

Bacterial strain and culture condition

Amycolatopsis alba JCM 10030 (type strain) was obtained from the Japan Collection of Microorganisms (JCM) Microbe Division at the RIKEN BioResource Center. The iron deficient medium was prepared by adding 2g of K_2SO_4, 3g of K_2HPO_4, 1g of NaCl, 5g of NH_4Cl in 1 L of deionized water. To remove ferric ions, the solution (1 L) was stirred with 50g of weakly acidic cation exchange resin Chelex-100 sodium form (Bio-rad, CA, USA) for 2 h. The solution was filtrated with paper filter (Whatman No.1, GE Healthcare Life Sciences, Buckinghamshire, England) and added with 80 mg of $MgSO_4$, followed by autoclaving. The separately sterilized solutions (10 mL each) of $CaCl_2$•H_2O (10 mg/mL), glucose (250 mg/mL), and 0.5% yeast extract (Difco) were added to 1L of sterile medium in clean bench. *A. alba* was cultured by total 2 L of iron-deficient media with incubated rotary shaker (100 rpm, 30 °C) for 7 days.

Isolation of albachelin

The culture medium of *A. alba* was harvested by filtering with paper filter to remove bacterial cells (Whatman No.1). The medium was added with 0.5 mL of 1M $FeCl_3$ and evaporated using rotary evaporator to concentrate to 50 mL of the final volume. The concentrated solution was subjected to open column chromatography with hydrophobic resin CHP20P (Mitsubishi Chemical, Tokyo, Japan) eluted with 10% MeOH, 60% MeOH, and MeOH. The 60%MeOH fraction was concentrated and repeatedly subjected to HPLC purification to obtain 8.2 mg of ferri-albachelin using C18 column (4.6× 250 mm, Wakopak Handy-ODS, WAKO, Osaka, Japan), eluted with 2% MeCN/98%water containing 0.05%TFA at a flow rate of 1 mL/min and monitored at UV-VIS absorbance 435 nm.

Conversion of ferri-albachelin into Ga-albachelin via desferri-albachelin

Ferri-albabachelin (6.0 mg) was dissolved in 3 mL of water. The solution was mixed with 3 mL of 1M 8-quinolinol and stirred at room temperature for 30 min Total 2 times of the two layer partition were performed using 6 mL of CH_2Cl_2 each time to get rid of ferri-8 quinolinol. The water layer was immediately collected and lyophilized by freeze-dryer. After dissolving the dry material in 2 mL of water, HPLC purification was performed using C18 column (4.6 × 250 mm, Wakopak Handy-ODS), eluted with 4% MeCN/96%water containing 0.05%TFA at a flow rate of 1 mL/min, and monitored at UV-VIS absorbance 215 nm to yield 6.0 mg of desferri-albachelin. Desferri-albachelin (5.0 mg) was dissolved in 2 mL of distilled water, and 10 mg of Gallium chloride (Sigma Aldrich, MO, USA) was added to convert it to Ga-albachlin. After HPLC purification in the same conditin as described above, 4.0 mg of Ga-albachelin was obtained.

NMR experiments

A NMR sample was prepared by dissolving the purified peptide in 500 μl of DMSO-d_6 (Sigma Aldrich). 1D ^{1}H, ^{13}C, DEPT-135, and all 2D NMR spectra were obtained on Bruker Avance800 spectrometer with quadrature detection (Bruker BioSpin, MA, USA). The 1D ^{1}H, ^{13}C, DEPT-135 spectra were recorded at 25°C with 15 ppm for proton and 240 ppm for carbon. The following 2D ^{1}H-NMR spectra were recorded at 25°C with 10 ppm or 15 ppm spectral widths in *t1* and *t2* dimensions in the phase-sensitive mode by States-TPPI method: two-dimensional (2D) double quantum filtered correlated spectroscopy (DQF-COSY), recorded with 512 and 2048 complex points in *t1* and *t2* dimensions; 2D homonuclear total correlated spectroscopy (TOCSY) with MLEV-17 mixing sequence, recorded with mixing time of 80 ms, 256 and 1024 complex points in *t1* and *t2* dimensions; 2D nuclear Overhauser effect spectroscopy (NOESY), recorded with mixing time of 200 ms, 512 and 2048 complex points in *t1* and *t2* dimensions. Water suppression was performed using presaturation method. 2D ^{1}H-^{13}C heteronuclear single quantum correlation (HSQC) and heteronuclear multiple bond connectivity (HMBC) spectra were acquired at 25°C in the echo-antiecho mode or in the absolute mode, respectively. The ^{1}H-^{13}C HSQC and HMBC spectra were recorded with 1024 × 512 complex points for 12 ppm in the ^{1}H dimension and 170 ppm in the ^{13}C dimension or for 10 ppm in the ^{1}H dimension and 220 ppm in the ^{13}C dimension, respectively, at a natural isotope abundance. 2D ^{1}H-^{15}N HSQC spectrum was also recorded at 25°C with 1024 × 64 complex points for 12 ppm in the ^{1}H dimension and 50 ppm in the ^{15}N dimension in the phase-sensitive mode by States-TPPI method at natural isotope abundance. All NMR spectra were processed using XWINNMR (Bruker). Before Fourier transformation, the shifted sinebell window function was applied to *t1* and *t2* dimensions except for the HMBC spectrum. All ^{1}H and ^{13}C dimensions were referenced to DMSO-d_6 at 25 °C.

MS experiments

All mass spectra were recorded in the positive-ion mode. ESI-TOF MS spectra of Ferri-albachelin and Ga-albachelin were recorded using a JEOL JMS-T100LP mass spectrometer (JEOL Ltd., Tokyo, Japan). The accurate mass of desferri-albachelin was analyzed using an ESI Fourier-transform ion cyclotron resonance (FT-ICR) mass spectrometer (Apex II 70e, Bruker Daltonics, MA, USA) and the MS/MS spectrum was recorded on a MALDI-TOF mass spectrometer (4800 plus TOF/TOF Analyzer, AB SCIEX, CA, USA) using α-cyano-4-hydroxy cinnamic acid (Bruker Daltonics) as the matrix. The mass spectrometers were tuned and calibrated using commercially available standard compounds such as "YOKUDELNA" (JEOL, Tokyo, Japan) for the FT-ICR mass analysis and a "Peptide Calibration Standard II" (Bruker Daltonics) for MALDI-TOF mass analyses prior to the measurement.

Modified Marfey method

Ferri-albachelin (1.0 mg) was subjected to acid hydrolysis at 105 °C for 16 h with concentrated HI (0.5 mL, WAKO), and the hydrolysate was dried by freeze-dryer and resuspended in H_2O (200 μL). To the hydrolysate, 10 μL of a solution of *N*α-(5-fluoro-2,4-dinitrophenyl)-L-leucinamide (L-FDLA, Sigma-Aldrich) or D-FDLA (Sigma-Aldrich) in acetone was added at the concentration of 10 mg/ml and 100 μL of 1 M $NaHCO_3$, after which the mixtures were heated to 80 °C for 3 min. The reaction mixtures were cooled, neutralized with 2 N HCl (50 μL), and diluted with MeCN (200 μL). About 20 μL of each solution of FDLA derivatives was subjected to HPLC analysis with C18 column (Wakopak Handy-ODS, WAKO, 4.6 × 250 mm). The DAD detector (MD-2018, JASCO, Tokyo, Japan) was used for detection of the amino acid derivatives accumulating the data of the absorbance from 220nm to 420 nm. The HPLC analysis for Ser was performed at a flow rate of 1 mL/min using solvent A (distilled water containing 0.05% TFA) and solvent B (MeCN containing 0.05%TFA) with a linear

gradient mode from 0 min to 60 min, increasing percentage of solvent B from 25% to 35% . The retention times (min) of L- or D-FDLA derivatized amino acids in this HPLC condition were following; L-Ser-L-FDLA (44.6 min), L-Ser-D-FDLA (46.2 min). The HPLC analysis for Orn and *N*-Me Orn was performed at a flow rate of 1 mL/min using solvent A (distilled water containing 0.05% TFA) and solvent B (MeCN containing 0.05%TFA). The isocratic mode was applied for first 20 min with elution of 27% of solvent B, and for next 20min, a linear gradient mode was applied, increasing percentage of solvent B from 27% to 30% . The retention times (min) of L- or D-FDLA derivatized amino acids in this HPLC condition were following; L-Orn-L-FDLA (34.4 min), L-Orn-D-FDLA (17.5 min), L-*N*-Me Orn-L-FDLA (31.5 min), L-*N*-Me Orn-D-FDLA (29.9 min).

Acknowledgement

This study was supported by the Japan Society for the Promotion of Science by Grants-in-aids (grant number 25350964).

Conflict of interest

The authors had no conflict of interest in undertaking this project.

References

Ahmed E, Holmstrom SJ (2014) Siderophores in environmental research: roles and applications. Microb Biotechnol 7:196-208 doi:10.1111/1751-7915.12117

Bachmann BO, Ravel J (2009) Chapter 8. Methods for in silico prediction of microbial polyketide and nonribosomal peptide biosynthetic pathways from DNA sequence data. Methods Enzymol 458:181-217 doi:10.1016/S0076-6879(09)04808-3

Barona-Gomez F, Wong U, Giannakopulos AE, Derrick PJ, Challis GL (2004) Identification of a cluster of genes that directs desferrioxamine biosynthesis in *Streptomyces coelicolor* M145. J Am Chem Soc 126:16282-16283 doi:10.1021/ja045774k

Challis GL (2005) A widely distributed bacterial pathway for siderophore biosynthesis independent of nonribosomal peptide synthetases. Chembiochem : a European journal of chemical biology 6:601-611 doi:10.1002/cbic.200400283

Challis GL, Ravel J (2000) Coelichelin, a new peptide siderophore encoded by the *Streptomyces coelicolor* genome: structure prediction from the sequence of its non-ribosomal peptide synthetase. FEMS Microbiol Lett 187:111-114

Challis GL, Ravel J, Townsend CA (2000) Predictive, structure-based model of amino acid recognition by nonribosomal peptide synthetase adenylation domains. Chem Biol 7:211-224

Clardy J (2006) Stopping trouble before it starts. ACS Chem Biol 1:17-19 doi:10.1021/cb0600029

Crosa JH, Walsh CT (2002) Genetics and assembly line enzymology of siderophore biosynthesis in bacteria. Microbiol Mol Biol Rev 66:223-249

329 Harada KI, Fujii K, Hayashi K, Suzuki M, Ikai Y, Oka H (1996) Application of D,L-FDLA
330 derivatization to determination of absolute configuration of constituent amino acids in
331 peptide by advanced Marfey's method. Tetrahedron Lett 37:3001-3004
332 Kodani S et al. (2013a) Structure and biosynthesis of scabichelin, a novel tris-hydroxamate
333 siderophore produced by the plant pathogen *Streptomyces scabies* 87.22. Org Biomol
334 Chem 11:4686-4694 doi:10.1039/c3ob40536b
335 Kodani S, Kobayakawa F, Hidaki M (2013b) Isolation and structure determination of new
336 siderophore tsukubachelin B from *Streptomyces* sp. TM-74. Nat Prod Res 27:775-781
337 doi:10.1080/14786419.2012.698412
338 Komaki H et al. (2014) Genome based analysis of type-I polyketide synthase and nonribosomal
339 peptide synthetase gene clusters in seven strains of five representative *Nocardia* species.
340 BMC genomics 15:323 doi:10.1186/1471-2164-15-323
341 Komaki H, Ichikawa N, Oguchi A, Hanamaki T, Fujita N (2012) Genome-wide survey of
342 polyketide synthase and nonribosomal peptide synthetase gene clusters in *Streptomyces*
343 *turgidiscabies* NBRC 16081. J Gen Appl Microbiol 58:363-372
344 Lautru S, Deeth RJ, Bailey LM, Challis GL (2005) Discovery of a new peptide natural product
345 by *Streptomyces coelicolor* genome mining. Nat Chem Biol 1:265-269
346 doi:10.1038/nchembio731
347 Lazos O, Tosin M, Slusarczyk AL, Boakes S, Cortes J, Sidebottom PJ, Leadlay PF (2010)
348 Biosynthesis of the putative siderophore erythrochelin requires unprecedented crosstalk
349 between separate nonribosomal peptide gene clusters. Chem Biol 17:160-173
350 doi:10.1016/j.chembiol.2010.01.011

351 Mercier A, Labbe S (2010) Iron-dependent remodeling of fungal metabolic pathways associated
352 with ferrichrome biosynthesis. Appl Environ Microbiol 76:3806-3817
353 doi:10.1128/AEM.00659-10
354 Ochi K, Hosaka T (2013) New strategies for drug discovery: activation of silent or weakly
355 expressed microbial gene clusters. Appl Microbiol Biotechnol 97:87-98
356 doi:10.1007/s00253-012-4551-9
357 Park HM et al. (2013) Genome-based cryptic gene discovery and functional identification of
358 NRPS siderophore peptide in *Streptomyces peucetius*. Appl Microbiol Biotechnol
359 97:1213-1222 doi:10.1007/s00253-012-4268-9
360 Robbel L, Knappe TA, Linne U, Xie X, Marahiel MA (2010) Erythrochelin -a hydroxamate-type
361 siderophore predicted from the genome of *Saccharopolyspora erythraea*. FEBS J
362 277:663-676 doi:10.1111/j.1742-4658.2009.07512.x
363 Rottig M, Medema MH, Blin K, Weber T, Rausch C, Kohlbacher O (2011) NRPSpredictor2 -a
364 web server for predicting NRPS adenylation domain specificity. Nucleic Acids Res
365 39:W362-367 doi:10.1093/nar/gkr323
366 Seyedsayamdost MR, Traxler MF, Zheng SL, Kolter R, Clardy J (2011) Structure and
367 biosynthesis of amychelin, an unusual mixed-ligand siderophore from *Amycolatopsis* sp.
368 AA4. J Am Chem Soc 133:11434-11437 doi:10.1021/ja203577e
369 Sieber SA, Marahiel MA (2005) Molecular mechanisms underlying nonribosomal peptide
370 synthesis: approaches to new antibiotics. Chem Rev 105:715-738 doi:10.1021/cr0301191
371 Zerikly M, Challis GL (2009) Strategies for the discovery of new natural products by genome
372 mining. Chembiochem : a European journal of chemical biology 10:625-633
373 doi:10.1002/cbic.200800389

374 Figure legends

375 **Fig. 1** Chemical structure of desferri-albachelin (**1**)

376 **Fig. 2** a) Key TOCSY, NOESY, and HMBC correlations of **1**, b) ESI-MS/MS analyses of **1**

377 **Fig. 3** Putative albachelin biosynthetic gene cluster and proposed pathway for albachelin
378 synthesis. (a) Organization of the albachelin biosynthesis gene cluster in *A. alba*. The proposed
379 functions of the protein encoded by the gene cluster are summarized in Table S1. (b) Proposed
380 role of enzymes encoded by AMYAL _RS0130200 to AMYAL_RS0130210 in the biosynthesis
381 of albachelin. Capital letters A, C, E, and MT represent adenylation, condensation, epimerization,
382 and methylation domains. Black filled circle represents a peptidyl carrier protein (PCP) domain.
383

384 Figure 1

385

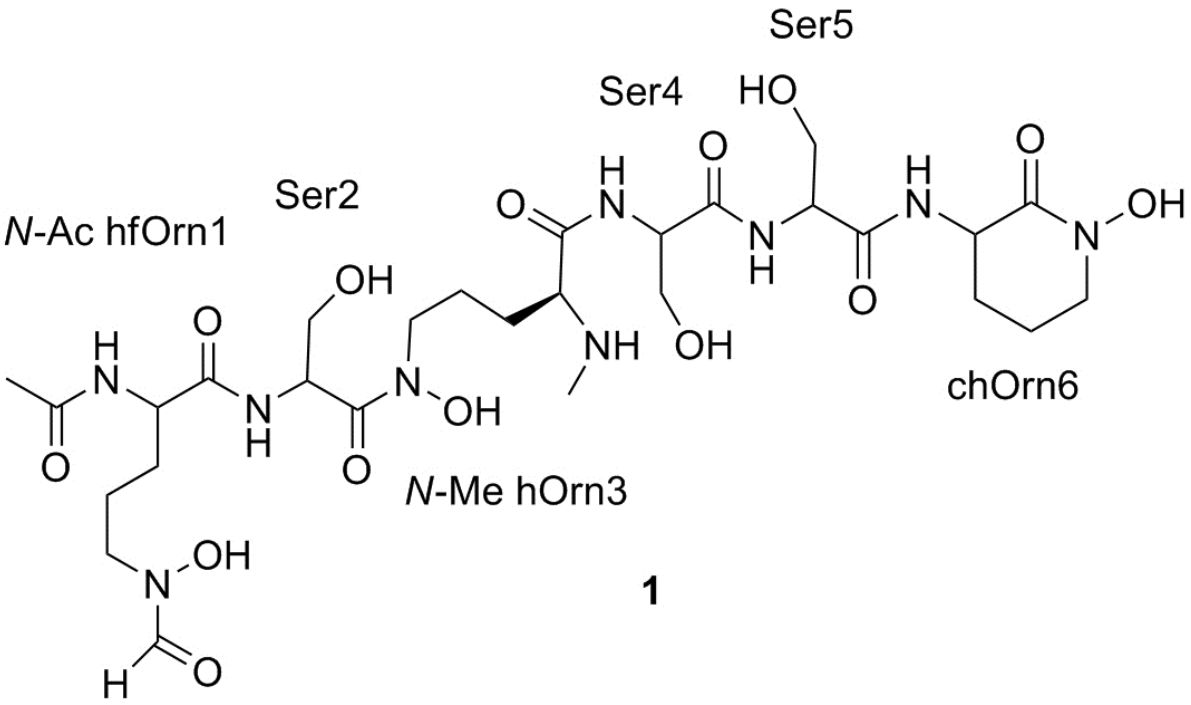

386 Figure 2

387

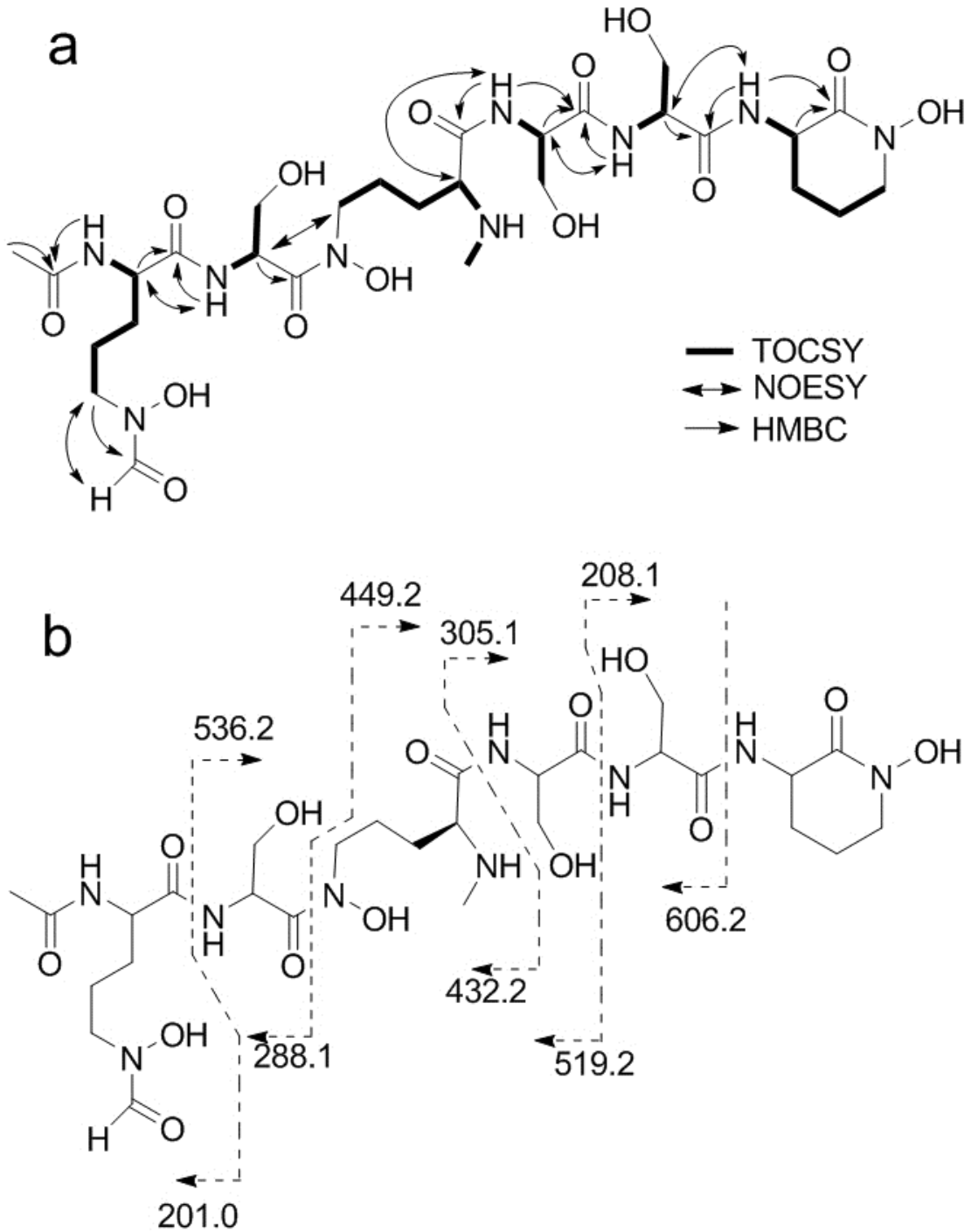

388 Figure 3

389 a

390 

b

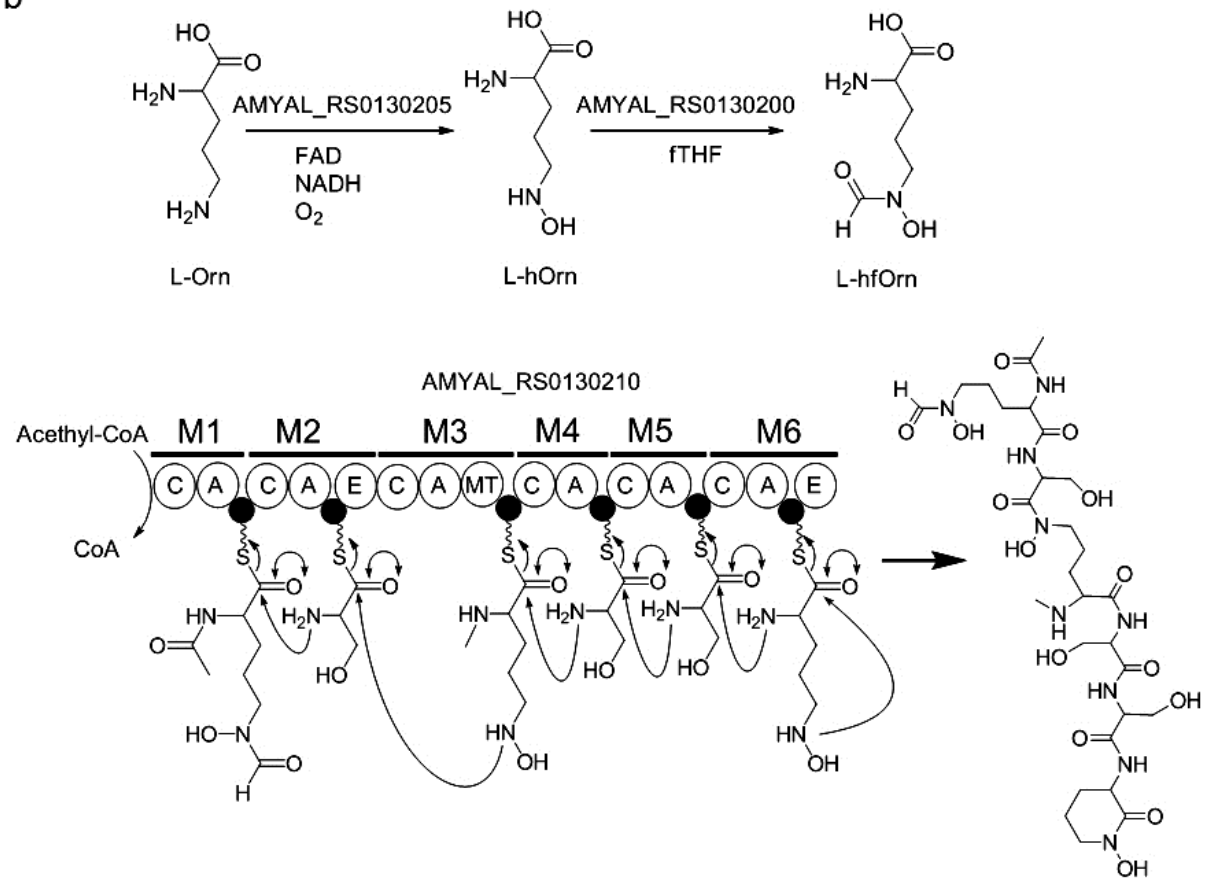

391 Table 1. NMR chemical shift values of Ga-albachelin in DMSO-d_6

Residue	Position	δH (*J* = Hz)	δC
N-Ac hfOrn1	*N*-Ac-CH_3	1.83 (s)	22.2
	N-Ac-CO		169.1
	NH	7.62 (d, 7.5)	
	CO		170.9
	α	4.43 (m)	50.7
	β	1.39 (m)	27.5
		1.52 (m)	
	γ	1.39 (m)	18.1
		1.50 (m)	
	δ	3.29 (m)	50.1
		3.49 (m)	
	formyl	7.99 (s)	152.2
Ser2	NH	8.35 (m)	
	CO		161.5
	α	4.84 (td, 9.1, 6.1)	48.1
	β	3.46 (m)	60.4
		3.56 (m)	
N-Me hOrn3	*N*-CH_3	2.51 (m)	30.7
	NH	8.85 (br)	
	CO		166.8
	α	3.91 (br)	59.2
	β	1.78 (m)	26.6
		1.89 (m)	
	γ	1.73 (m)	22.3
		1.79 (m)	
	δ	3.53 (m)	49.5
		4.81 (m)	
Ser4	NH	8.67 (d, 8.4)	
	CO		169.0
	α	4.64 (m)	54.6
	β	3.51 (m)	61.8
		3.54 (m)	
Ser5	NH	8.36 (m)	
	CO		169.8
	α	4.41 (m)	53.8
	β	3.42 (m)	60.8
		3.58 (m)	
chOrn6	NH	8.34 (d, 8.4)	
	CO		159.5
	α	4.62 (m)	44.9
	β	1.66 (m)	26.4
		1.96 (m)	
	γ	1.81 (m)	18.4
		2.12 (m)	
	δ	3.58 (m)	49.5

392

393